# BEAM-AUGMENTED SPACE-TIME ADAPTIVE PROCESSING

*Yaron Seliktar* [1,2] *Douglas B. Williams* [1] *E. Jeff Holder* [2]

[1]Center for Signal and Image Processing, School of ECE, Georgia Institute of Technology, Atlanta, GA USA
[2]Georgia Tech Research Institute, Georgia Institute of Technology, Atlanta, GA USA

## ABSTRACT

Combined monostatic clutter (MSC) and terrain scattered interference (TSI) pose a difficult challenge for adaptive radar processing. Mitigation techniques exist for each interference alone but are insufficient for their combined effects. Current approaches separate the problem into two stages where TSI is suppressed first and then MSC. The problem with this cascade approach is that during the initial TSI suppression stage, the MSC becomes corrupted. In this paper an innovative technique is introduced for achieving a significant improvement in cancellation performance for both MSC and TSI, even when the jammer appears in the mainbeam. The majority of the interference rejection, both TSI and MSC, is accomplished with an MSC filter, with further TSI suppression accomplished via an additional tapped reference beam. Simultaneous optimization of the MSC filter weights and reference beam weights yields the desired processor. Performance results using Mountaintop data demonstrate the superiority of the proposed processor over existing processors.

## 1. INTRODUCTION

For modern pulsed airborne radars the availability of spatial information and two kinds of temporal information, slow-time and fast-time, is necessary in order to detect targets in the presence of strong interference. Primary sources of interference include monostatic clutter (MSC) caused by the reflections of radar signals from the surrounding terrain, direct path jamming, and possible multipath jamming components known as hot clutter or terrain scattered interference (TSI). Returns containing MSC are correlated in space and slow-time, whereas returns containing TSI are correlated in space and fast-time.

Different processing techniques are available to make use of the multi-dimensional data returns received and sampled by the radar for interference cancellation. Conventional (non-adaptive) processing, although simple and computationally efficient, fails to provide adequate suppression of interference in a realistic clutter and jamming environment. Adaptive algorithms, especially partially adaptive algorithms that exploit the correlation structure of the interference, offer a practical and high performance alternative to conventional processing. Space/slow-time adaptive processing (STAP), is suitable for rejecting MSC and jamming signals [4], whereas processing in space and fast-time is suitable for rejecting TSI and jamming signals [1, 2]. While, STAP and space/fast-time adaptive processing techniques cope well with MSC and TSI individually, neither type of processing is effective for the combined effects of MSC and TSI.

Mitigation of combined TSI and MSC requires processing in three dimensions. A fully adaptive three dimensional processor, however, is impractical and therefore reduced rank alternatives must be sought. The Factored Beamspace Algorithm (FBA) in [2] is one such reduced rank algorithm that is specifically designed for the combined MSC and TSI problem. The idea is to first remove TSI from the data using a space/fast-time processor and then feed the "TSI free" data to a STAP processor. Drawbacks of this factored approach, such as MSC distortion [3] and the requirement of "clutter free" training data, motivate us to investigate alternatives. In this paper, we introduce an innovative technique for achieving a significant improvement in interference cancellation performance over both STAP and the Factored Beamspace approach.

## 2. SPACE-TIME PROCESSING

Considered here is a radar system that transmits a sequence of $M$ coherent pulses and samples the returns on an $N$ element uniform linear array.[1] It collects $L$ temporal samples from each element receiver at each *pulse repetition interval (PRI)*, where each time sample corresponds to a *range cell*. The three-dimensional datacube structure depicted in Figure 1 represents the sampled returns in a single *coherent processing interval (CPI)* of $M$ pulses. This set of samples is denoted by a sequence of $M$ matrices $\mathbf{X}^{(m)}$(i.e., one for each pulse) with elements $x^{(m)}(n,l)$. To distinguish between temporal dimensions, the inter-PRI sampling dimension is referred to as *slow-time* (abbreviated *stime*) and the range cell dimension as *fast-time* (abbreviated *ftime*). The element and slow-time dimensions are typically denoted in the frequency domain as spatial frequency ($\nu$) and Doppler ($f$), respectively. From Figure 1, a spatial snapshot consists of $N$ elements of spatial data from the $t^{th}$ range cell (i.e., $t^{th}$ column of $\mathbf{X}^{(m)}$),

$$\mathbf{x}^{(m)}(t) = \begin{bmatrix} x^{(m)}(0,t) \\ x^{(m)}(1,t) \\ \vdots \\ x^{(m)}(N-1,t) \end{bmatrix}. \tag{1}$$

A space-stime snapshot consists of stacked element data from consecutive pulses at a given range cell and is denoted

This work was partially supported by Wright Labs, USAF. Computing facilities used in this research are supported in part by the NSF under Grant MIP-9295853 and the Hewlett-Packard Company.

[1]In the notation here, $N$ denotes a scalar constant, $\mathbf{n}$ a spatial vector, and $\mathbf{N}$ a space-time vector or matrix.

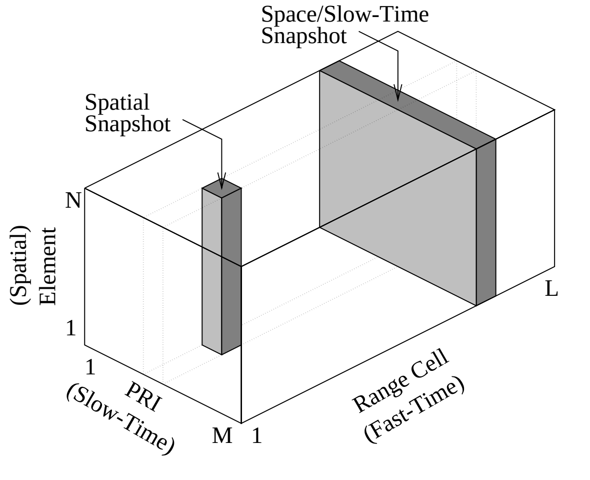


**Figure 1**: Datacube.

by

$$\mathbf{X}(t) = \begin{bmatrix} \mathbf{x}^{(0)}(t) \\ \mathbf{x}^{(1)}(t) \\ \vdots \\ \mathbf{x}^{(M-1)}(t) \end{bmatrix}. \quad (2)$$

The two-dimensional space-stime steering vector steered in the direction of the desired normalized Doppler and spatial frequency pair ($\hat{f}$,$\nu$) is defined as

$$\mathbf{v} = \mathbf{v}(\hat{f}, \nu) = \mathbf{b}(\hat{f}) \otimes \mathbf{a}(\nu). \quad (3)$$

Assuming a uniform linear array and fixed PRI, the spatial and temporal steering vectors are defined respectively as

$$\mathbf{a}(\nu) = \frac{1}{\sqrt{N}} \begin{bmatrix} 1 & e^{j2\pi\nu} & \cdots & e^{j2\pi\nu(N-1)} \end{bmatrix}^T, \quad (4)$$

$$\mathbf{b}(\hat{f}) = \frac{1}{\sqrt{M}} \begin{bmatrix} 1 & e^{j2\pi\hat{f}} & \cdots & e^{j2\pi\hat{f}(M-1)} \end{bmatrix}^T, \quad (5)$$

where superscript T denotes the transpose operator. The spatial frequency $\nu$ is related to azimuth angle, $\phi$, by $\nu = \frac{D}{\lambda}\sin(\phi)$, where $D$ is the inter-element spacing of the array and $\lambda$ is the radar's operating wavelength [1]. The normalized Doppler frequency is $\hat{f} = fT_r$ where $T_r$ is the PRI.

The output of a linear time-invariant processor can be expressed as the inner product of a weight vector, $\mathbf{W}$, and the input vector, $\mathbf{Y}(t)$,

$$z(t) = \mathbf{W}^H\mathbf{Y}(t), \quad (6)$$

where superscript H denotes the complex conjugate transpose operator. The vector quantity $\mathbf{Y}(t)$ represents the input to the processor and is defined according to the type of processing employed.

Adaptive processing typically requires solving for a set of weights, $\mathbf{W}$, that is optimal in the mean square sense. In other words, the mean square output of the processor,

$$\zeta = E\left\{|z(t)|^2\right\} = E\left\{\mathbf{W}^H\mathbf{Y}\mathbf{Y}^H\mathbf{W}\right\} = \mathbf{W}^H\mathbf{R}_{\mathbf{Y}}\mathbf{W}, \quad (7)$$

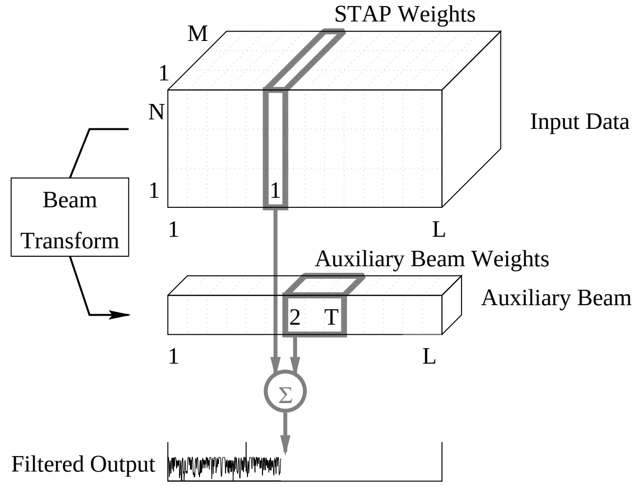


**Figure 2**: Beam Augmented STAP architecture.

is minimized with respect to $\mathbf{W}$ subject to the constraints $\mathbf{C}\mathbf{W} = \mathbf{c}$. The solution can be expressed in closed form as

$$\mathbf{W} = \mathbf{R}_{\mathbf{Y}}^{-1}\mathbf{C}^H\left(\mathbf{C}\mathbf{R}_{\mathbf{Y}}^{-1}\mathbf{C}^H\right)^{-1}\mathbf{c}. \quad (8)$$

When computing weights for a STAP processor, the constraints are typically selected so as to satisfy a unity gain condition at the desired Doppler and look angle (i.e., $\mathbf{W}^H\mathbf{v}(\hat{f}, \nu) = 1$).

## 3. BEAM-AUGMENTED STAP

Experimental results on Mountaintop[2] (MT) data show that STAP does not perform as poorly as suspected in combined interference environments. This result is not altogether surprising since the major sources of interference are MSC and direct path jamming, which can be removed through STAP. Furthermore, TSI can be partially mitigated with spatial processing. Based on this result, the proposed architecture has as its principal component, a fully adaptive STAP processor. The spatial-stime processing performed by the STAP processor can then accomplish significant spatial nulling of the jammer and MSC. On the other hand, fast-time processing, expected to provide only marginal improvement in cancellation performance, is auxiliary and, therefore, need not be allotted the same degree of flexibility as the STAP processor. Consequently, for the proposed approach, fast-time taps are applied only to a single beam formed in space and slow-time, rather than to individual pulses and elements. Such a filter mechanism is illustrated in Figure 2. In this architecture, $MN$ weights are applied to all elements and pulses in the first tap (STAP weights). Additionally, an auxiliary beam in angle and Doppler is formed and weights are applied to $T-1$ fast-time taps of that beam. The auxiliary beam is defined as

$$\mathbf{A}(t)^T = \mathbf{F}^H \begin{bmatrix} \mathbf{X}(t-1) & \cdots & \mathbf{X}(t-T+1) \end{bmatrix}, \quad (9)$$

where $\mathbf{F} = \mathbf{v}(\hat{f}, \nu)$ is a conventional, nonadaptive spatial/Doppler beamformer. In the equation relating output

[2]See URL `www.mhpcc.edu` for information on Mountaintop datasets.

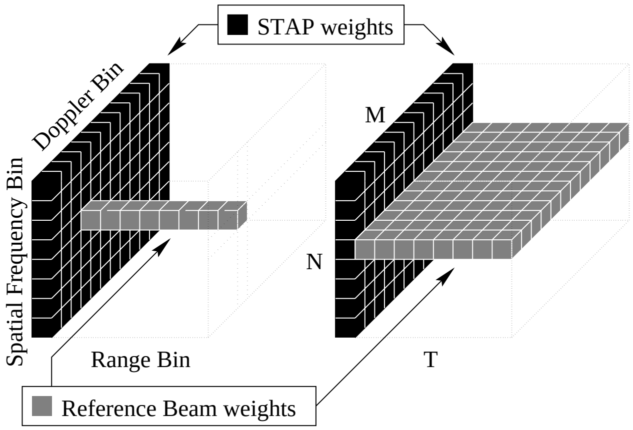


**(a) Single Beam BASTAP** **(b) Multiple Beam BASTAP**

**Figure 3**: Beamspace interpretation of BASTAP.

to input (6) the input vector, $\mathbf{Y}(t)$, is defined as

$$\mathbf{Y}(t) = \begin{bmatrix} \mathbf{X}(t) \\ \mathbf{A}(t) \end{bmatrix}. \tag{10}$$

With a filter architecture at hand, an adaptation scheme is required. It is most straight forward to optimize all the weights simultaneously using Eq. 8 and apply a set of constraints to achieve the desired response characteristics. Since both sets of STAP weights and auxiliary fast-time weights are optimized together, STAP performance can only be enhanced and there is no concern that fast-time processing comes at the expense of STAP processing.

An interpretation of this approach utilizing beamspace data is illustrated in Figure 3a. A two-dimensional DFT is applied across elements and PRIs at each range cell. Weights (shown in black) are then applied across all spatial and Doppler bins from the first tap, i.e., the STAP portion of the processor. Fast-time weights are then applied across $T-1$ taps from a single selected beam represented by the gray shaded cubes.

BASTAP need not be restricted to a single beam. Multiple beams can be used to enhance performance in the presence of nonstationary TSI, such as that present in airborne radar data. In fact, such TSI has correlation not only in fast-time but also in slow-time. Thus, it is necessary to apply beams across all Doppler bins from a single spatial frequency bin, as depicted in Figure 3b. In such a case, $Y(t)$ is defined as above in (10), with the beam transformation $\mathbf{F}$ having multiple spatial/Doppler filters:

$$\mathbf{F} = \begin{bmatrix} \mathbf{v}(\hat{f}_0, \nu_0) & \mathbf{v}(\hat{f}_1, \nu_1) & \cdots & \mathbf{v}(\hat{f}_{N_b}, \nu_{N_b}) \end{bmatrix}. \tag{11}$$

## 4. SIMULATION RESULTS

Performance results for BASTAP were obtained for MT dataset `mmit004v1` containing a direct path jammer at 32° and stationary TSI, and for MT dataset `hot6067v1` containing a direct path jammer at $-2°$ and nonstationary TSI. In both instances datasets were combined with 40 dB of synthetic MSC and injected with a 50 dB synthetic target with a $-100$ Hz Doppler shift. The three processors considered were BASTAP, fully adaptive STAP, and FBA.

| TSI dataset | $\phi_{look}$ | BASTAP | STAP | FBA |
|---|---|---|---|---|
| `mmit004v1` | 0 | 11.7 dB | 17.5 dB | 18.0 dB |
| `mmit004v1` | 32 (MBJ) | 24.2 dB | 31.3 dB | 28.9 dB |
| `hot6067v1` | 30 | 21.0 dB | 27.3 dB | 20.7 dB |
| `hot6067v1` | -2 (MBJ) | 29.9 dB | 37.7 dB | 30.2 dB |

**Table 1**: Summary of OINR results for regular and mainbeam jamming (MBJ).

### 4.1. Stationary TSI

In analyzing the three processors on stationary TSI data, the assumed target direction and Doppler were 0° and $-100$ Hz. BASTAP was configured with a 99-tap reference beam pointed at the jammer (i.e., 32°) and tuned to $-100$ Hz. FBA was configured with 25 taps in the first stage and a fully adaptive STAP processor in the second. For these configurations BASTAP totaled 323 adaptive weights, STAP 224 adaptive weights, and FBA had 350 adaptive weights in the first stage and 224 adaptive weights in the second stage. Figure 4 shows the outputs of the conventional and adaptive processors. All three adaptive processors unmasked the 50 dB target at range bin 500, with BASTAP achieving the best cancellation performance. With a residual output interference to noise ratio (OINR) of 11.7 dB, BASTAP improved over STAP by 5.8 dB and over FBA by 6.3 dB. In a more difficult case of mainbeam jamming where the target was obscured by the direct path jammer (i.e., at 32°), referring to the results in Table 1, BASTAP at 24.2 dB still offered an improvement of 7.1 dB over STAP and 4.7 dB over FBA.

Figure 5 illustrates OINR performance for BASTAP having between 1 and 300 taps. For the ordinary jamming case (solid line) roughly 14 dB of improvement was attained in going from 1 tap (i.e., STAP) to 300 taps. Most of the curve is fairly flat with sharp drop offs occurring at roughly 50 and 140 taps. Thus, a majority of the cancellation can be achieved by incorporating only a select number of taps. A priori determination of these taps could result in computational savings and a reduction in the required sample support. In contrast to ordinary jamming, however, mainbeam jamming (dashed line) does not have the sharp drop offs necessary to consider weight thinning strategies. Furthermore, in going from 1 to 300 taps, only 10 dB of improvement was attained.

The beampattern responses of BASTAP and FBA are three dimensional; however, two-dimensional cross-sectional slices are sufficient to indicate the behavioral response of the processors. The top of Figure 6 shows the space-Doppler cross-section at the zeroth lag for BASTAP and FBA. The response of BASTAP shows improvement over that of FBA, as discerned by the reduced gain in regions away from the target's look direction (0°) and Doppler frequency ($-100$ Hz). Both responses have a visible monostatic clutter null cutting across diagonally. The mainbeam (at 0° and $-100$ Hz) can be discerned easily, although more clearly in the BASTAP response. At the bottom of Figure 6 is the space-ftime response of BASTAP and FBA shown for the first ten time taps at $-100$ Hz (i.e., target Doppler). The well-behaved response of BASTAP is characterized by the absence of target spreading and overall low gain in successive taps. The fact that FBA introduces excess gain throughout the space-ftime region and yet does not achieve the level of cancellation of BASTAP suggests

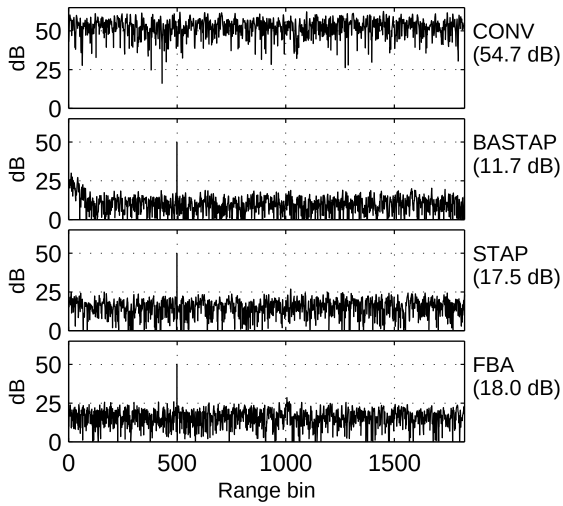


**Figure 4**: Filter outputs with OINR.

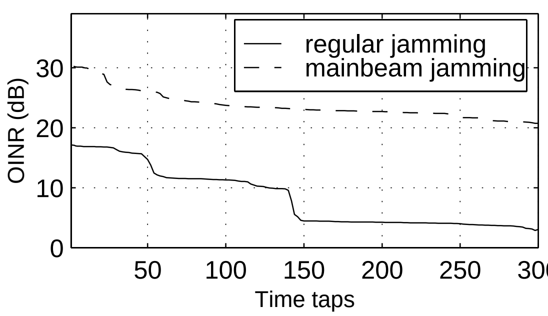


**Figure 5**: OINR vs. number of taps.

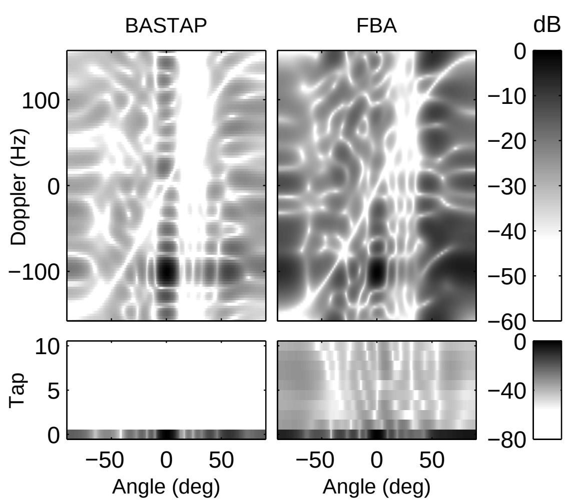


**Figure 6**: 2D Beampatterns.

that BASTAP is a more natural and efficient choice for the combined TSI, MSC, and mainbeam jamming problem.

### 4.2. Nonstationary TSI

Despite its clear advantage over FBA in the stationary case, BASTAP evens off in performance with FBA in the nonstationary case. In the nonstationary case the jammer multipath components that make up the composite TSI signal experience Doppler shifts from radar platform and jammer motion. The Doppler spread in the TSI necessitates Doppler compensation in BASTAP, and, therefore, a single reference beam at one select Doppler is no longer sufficient. In comparing processors, FBA was configured with 40 taps, while BASTAP was configured as shown in Figure 3b with sixteen 25-tap reference beams pointed at the jammer ($-2°$) and distributed evenly across the 312.5 Hz Doppler spectrum. The added Doppler beams come at the expense of reduced temporal taps. Table 1 demonstrates roughly equivalent performance for BASTAP and FBA for regular jamming and mainbeam jamming, however, both processors prove advantageous over plain STAP.

## 5. CONCLUSIONS

The main innovation introduced in this paper is a reduced rank technique for the joint mitigation of jamming, TSI, and monostatic clutter. It was demonstrated through a number of examples that the processor performs quite well under conditions of stationary TSI, offering improved cancellation and beampattern response performance over existing techniques. In the case of nonstationary TSI, BASTAP still maintained superiority over STAP but evened off with the factored beamspace approach. The investigation of BASTAP, however, is far from complete, in particular for the nonstationary case. The flexibility of beam selection and tap placement in BASTAP could potentially lead to improved BASTAP architectures. At present, beam selection strategies together with weight thinning strategies have not been considered. However, it is anticipated that further enhancements to BASTAP could come by considering these and other issues.

## 6. REFERENCES


[1] S. M. Kogon, D. B. Williams, E. J. Holder, "Beamspace Techniques for Hot Clutter Cancellation", *ICASSP 96*, vol. 2, pp. 1177-1180, May 1996.

[2] S. M. Kogon, *Adaptive Array Processing Techniques for Terrain Scattered Interference Mitigation*, Ph.D. Thesis, Georgia Institute of Technology, 1997.

[3] S. M. Kogon, E. J. Holder, D. B. Williams, "On the Use of Terrain Scattered Interference for Mainbeam Jammer Suppression," *ASAP 97*, March 1997.

[4] J. Ward, *Space-Time Adaptive Processing for Airborne Radar*, Technical Report 1015, MIT Lincoln Laboratory, 1994.

[5] Y. Seliktar, D. B. Williams, J. H. McClellan, "Evaluation of Partially Adaptive STAP Algorithms on the Mountain Top Data Set," *ICASSP 96*, vol. 2, pp. 1169-72, May 1996.